The Fourth International Workshop on
Micro and Nanotechnology for Power Generation
and Energy Conversion Applications
PowerMEMS 2004
November 28 - 30, 2004
Kyoto, Japan

Micromachined Silicon Structures for Free-Convection PEM Fuel Cell Power Sources

Dean Modroukas[1,2], Vijay Modi[1] and Luc Fréchette[3,1]
Power MEMS Conference
Columbia University, Rm. 220 S.W. Mudd, 500 West 120th Street, New York, NY 10027 USA
Tel 914-419-6330, dm274@columbia.edu
[1]Columbia University, [2]ATK GASL, and [3]Université de Sherbrooke

ABSTRACT

This paper presents details on the design, fabrication, testing and modeling of micromachined gas diffusion media (GDM) for micro PEM fuel cell applications. Two-tiered mesh structures were thru-etched into silicon wafers and subsequently installed and tested in a transparent, hydrogen-fueled test rig. These silicon structures supported a thermally evaporated gold current collection layer and were tested with commercially available membrane electrode assemblies (MEA's) of the "catalyst-on-membrane" variety. In general, the cell V-I performance curves approached that of conventional GDM but suffered from higher activation losses. While operating in free-convection mode, the cell operability became less stable at current densities >75mA/cm^2 and liquid water formation was observed in the micromachined cathode GDM. Single and two-phase flow modeling of the fuel cell operating in free-convection mode was also developed. Simulations support the experimental results and suggest that water accumulation significantly reduces the maximum current density achievable for such micro fuel cells.

Keywords: MEMS, micro-fuel cell, micro-PEM fuel cell, free-convection fuel cell, micro-power

I. INTRODUCTION

Two of the major challenges in the development and commercialization of small Proton-Exchange Membrane (PEM) fuel cell systems are (1) the miniaturization of the components that are used to engineer a fuel cell and (2) the reduction in the need for auxiliary components as they decrease the overall energy density and increase system complexity.

In order to achieve the first challenge, MEMS-based microfabrication techniques are employed to develop silicon-based structures that replace conventional current collectors and gas diffusion media (GDM). Microfabrication permits fine feature resolution, geometry optimization, porosity control, and management of wetting characteristics that are needed to develop micro fuel cell components. Over the past 5 years, a number of researchers have implemented microfabrication of silicon for micro fuel cell research and development. [1-3]

A significant contribution to balance of plant requirements is the need for small fans or pumps to provide forced convection of air and product water removal to and from the cathode of the fuel cell. We have addressed the second challenge, by operating these power sources in a free convection mode thus eliminating the need for these auxiliary components and associated controls. A key aspect to designing a robust, ambient air-breathing system is the fundamental understanding of the transport phenomena primarily present in the cathode of PEM fuel cells. Included in these transport processes is passive water removal which left unaddressed, results in obstruction of the catalytic sites.

This paper provides details on the design, fabrication, testing and modeling of micromachined GDM for small PEM fuel cell applications (<100W). Two-tiered mesh structures were thru-etched into silicon wafers and subsequently installed and tested in a transparent, hydrogen-fueled, single-cell test rig. These structures, due to their inherent rigidity, also served as support for a gold current collection layer. Commercially available membrane electrode assemblies (MEA's) of the "catalyst-on-membrane" variety were procured from *Ion Power, Inc.* and used for all tests. Furthermore, single and two-phase modeling of the fuel cell operation in free-convection mode was developed using the *FEMLAB* package and is presented below.

II. DEVICE DESIGN

Microfabrication Summary

The micromachined GDM elements were prepared using 50.8mm silicon wafers and were designed as a two-tiered mesh. The first mesh is a "coarse" 550μm × 550μm square mesh with supports ribs 150μm wide that are etched through 80% of the wafer thickness with a total area of 1cm^2. The second etch is also 1cm^2 with 55μm × 55μm square meshes having 15μm wide rib supports that are aligned to the coarser mesh. Two photolithographic masks were developed in order to pattern the two sets of meshes.

The micromesh GDM's were fabricated using well characterized microfabrication processes such as photolithography, deep reactive ion etching (DRIE), and thermal evaporation. The eleven basic fabrication steps that were performed during the fabrication process are given Figure 1 below. The starting material was a 50.8mm, 400μm thick double-side polished silicon wafer. *AZ4620* thick photoresist was patterned with the fine mesh geometry on the wafer using standard photolithographic techniques (steps 1-3). The wafer was bonded to a 101.6mm carrier wafer and was subsequently deep-etched in a *PlasmaTherm 770SLR* roughly 50μm deep (steps 4 and 5). The side walls of the silicon mesh structures were by default non-wetting due to Teflon® deposition during the passivation cycle of the deep etch thus simulating the hydrophobic characteristics of conventional GDM. The wafer was then backside patterned

with the coarse mesh geometry (steps 6-8) and subsequently deep etched through the wafer until the large pores exposed the fine pores (steps 9 and 10). Finally, the etched wafers were positioned in the thermal evaporator such that the fine mesh face received a 0.1μm chromium adhesion layer followed by roughly 1μm thick layer of 99.999% pure gold.

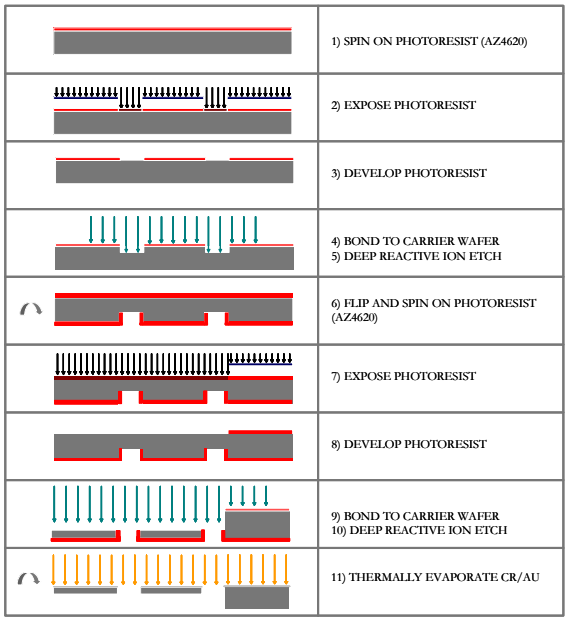

Figure 1: Process Flow

Figure 2 shows an SEM image of a device prior to the thermal evaporation of the gold current collection layer. The final device with Cr/Au current collection layer and soldered electrical leads is shown in the digital photograph of Figure 3. The inset picture in this same figure shows a top view zoom of the two-tiered micro GDM structure.

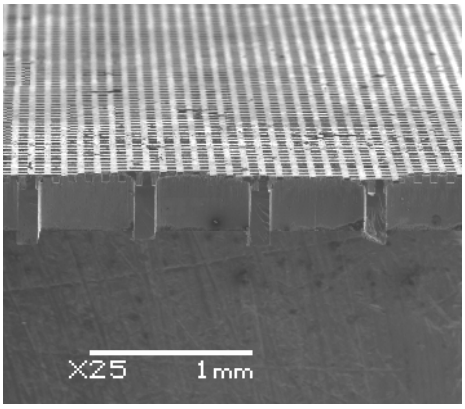

Figure 2: SEM Image of Cleaved Device

Assembly/Integration

After fabrication of the micro meshes, a 1cm^2 active area MEA prepared by Ion Power, Inc was sandwiched in between two silicon devices as shown in the assembly schematic of Figure 4. In this particular instance a conventional gas diffusion media cloth was utilized only on the anode side only for the sole purpose of serving as a compressible media that would help to even out the compressive loads and prevent mesh fracture.

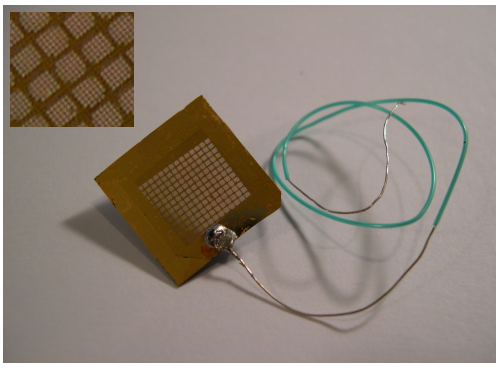

Figure 3: Digital Photograph of Final Micromachined GDM

Notice that the figure depicts an extended "tab" on one side of the structure to permit a soldered electrical connection that will not cause interference during assembly. It should be noted that due to solder runoff and insufficient "tab" area during cleaving, the cell was installed with only 80% of the mesh area in contact with MEA active area.

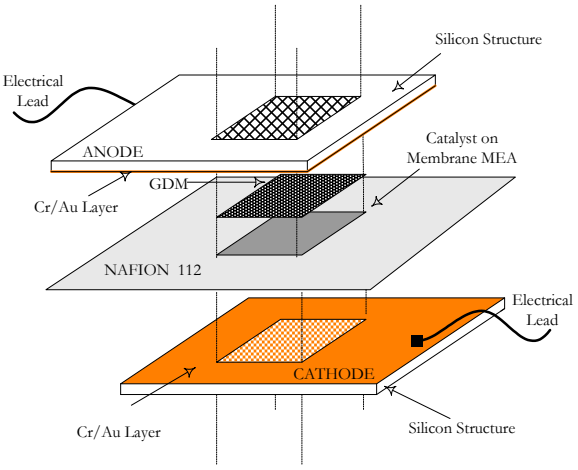

Figure 4: Schematic Depicting Cell Assembly*
*Note: Carbon Cloth GDM Used on Anode Side Only

Test Rig Details

The final cell assembly was installed into a single-cell, polycarbonate test rig depicted schematically in Figure 5 below. The key components to the rig are a set of 19mm thick polycarbonate endplates with integral seal grooves as well as gas entry and exit ports. The endplates are machined to accept a polycarbonate plug that sits above the face of the electrodes and current collector elements. Machined into each plug is a flowpath that coincides with the endplate's top and bottom gas entry and exit ports. Depending on whether the port is used or not, the cell is able to operate in either forced or free convection mode as shown schematically in Figure 5. In forced convection mode with the plug installed, a flowpath machined into the plug expands the inlet flow into a planar sheet that flows across the grid elements. In free convection mode the cathode plug is removed and the cell is exposed to ambient air.

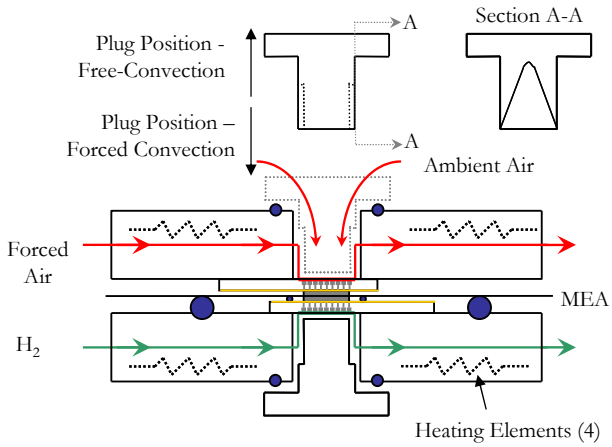

Figure 5: Schematic Depicting Cell Assembly

III. EXPERIMENTAL RESULTS

A *Lynntech Industries Inc.* test station was used for the experimental phase of the work. Table 1 below provides a summary of the test conditions.

Table 1 – Test Conditions & Test Stand Features

Oxidant	Ambient Air, Forced Air, Oxygen
Fuel	Hydrogen (15 sccm)
Cell Temperature	38°C (nominal)

Polarization Curves

The primary overall performance measure of a fuel cell is a cell polarization curve (termed V-I curve) that presents the overall cell (or stack) voltage as a function of current density. Cell polarizations alone provide a good deal of information to a fuel cell developer regarding his/her design. For example, open cell voltage and low current density data associated with activation or crossover losses can be identified and compared to existing designs. The slope of the V-I curves in the midrange current densities provides information on the total ohmic resistance present in the system. Finally, the V-I curve provides information on the cell's limiting current. The latter is a function of reactant or product mass transport resistances throughout the cell. [4]

Although the research focus is on device design for passive, ambient air-breathing systems, the cell was also tested in forced convection mode with both air and oxygen. IR-corrected polarization curves are shown in Figure 6 for the various operating modes and oxidant gases. Polarization data is also presented for a conventional test rig equipped with serpentine flowpaths and conventional carbon cloth gas diffusion media. In all cases the data presented in Figure 6 represent steady state operation defined by voltage time histories being constant for a minimum of 15 minutes per load setting. Known ohmic losses due to electrical connections and contact resistance between the layers of the cell are removed from all results for proper comparison.

Resistive losses due to insufficient contact forces limited the maximum current density that could be achieved and prevented testing the cell to its limiting current density. The MEMS-based fuel cell data (D005-550I) shows performance slightly less than that obtained with conventional gas diffusion media and serpentine flowfield with the primary difference being caused by activation overpotential. In general, the free-convection operation of the MEMS-based fuel cell showed stable performance at the lower current densities (<75mA/cm^2). At higher current densities, it is speculated that poor liquid water removal resulted in less stable operation. Figure 7 shows an SEM image of a large pore with the smaller pores showing signs of water flooding.

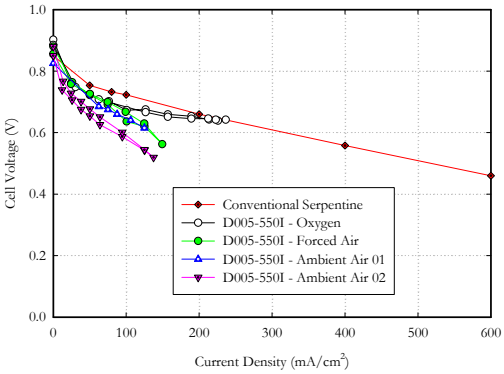

Figure 6: Polarization Data for Cell

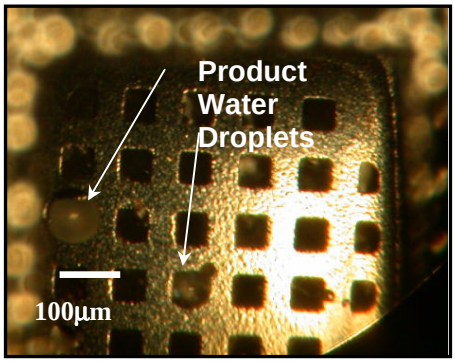

Figure 7: Stereoscopic Image of Single "Coarse" Pore During Test

Diagnostics

In addition to the polarization data, electrochemical impedance spectroscopic (EIS) measurements were taken at various cell operating points. The EIS results permitted accurate measurements of the ohmic losses due to contact resistances. Charge transfer or kinetic resistance was determined from the EIS measurements to be nearly four times more with the silicon GDM compared to the carbon cloth used in the conventional rig with the same MEA. This source of this effect is currently under closer examination; however, it quantitatively explains the larger activation loss between the silicon and carbon cloth GDM's.

IV. MODELING RESULTS

Along with the experimentation, single and two-phase simulations have been performed to model the transport processes of both the reactant air and product water. These simulations concentrated on free-convection mode of operation due to our research focus and the aforementioned advantages of simplicity and power of plant minimization.

Modeling Summary

Figure 8 shows the schematic of the modeled domain which consists of a single "pore" of the fine mesh of the silicon micromachined GDM. The boundary A-B represents the top of the fine mesh or equivalently, the bottom of the coarse mesh. The direction normal to the reactive surface (y direction) and the parallel dimension (x direction) across the face of the pore and current collector shoulder are modeled here. The model domain consists of half the width of the catalyst region (1) and half the width of the pore (2). In typical free-convection fuel cell operation, oxygen from the ambient air is supplied to the cathode primarily by diffusion and to a lesser extent through convection set up by a "suction-effect" or temperature induced velocity gradients. Water is generated at the electrode interface by the oxygen reduction reaction and net water migration through the membrane from the anode.

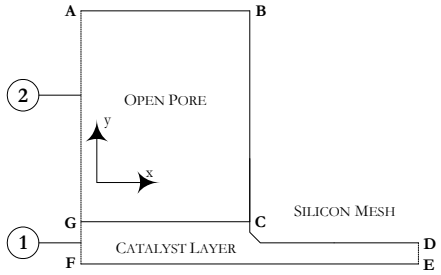

Figure 8: A Schematic of the Modeled Domain

Oxygen, water vapor and nitrogen gases are modeled throughout all domains using multi-component convection/diffusion relation termed the Maxwell-Stefan relations. Darcy's law for flow within porous media is implemented for both the gas and liquid phases for the catalyst layer and the incompressible form of the Navier Stokes equations is used to model the open "pore" region of the mesh. In general, the model was developed to permit simulations both with and without liquid saturation (i.e., water can exist as either gas only or as two phases). The free-convection boundary condition for A-B was set to a species flux that permitted species mass fractions to be calculated based on a prescribed mass transfer coefficient and far-field conditions.

Comparisons with Experimental Data

Figure 9 shows the model generated polarization curve with and without saturation effects compared to the experimental data. The modeling results show identical behavior up to 100mA/cm^2 with divergence at current densities greater than this value. Although we were unable to reach the cell's liming current condition, we feel the results obtained with saturation are more representative of the cell's performance since it became less stable at current densities >75mA/cm^2 where liquid water is present in both the experiment and two-phase model. In essence, the simulations without saturation represent a theoretical maximum to the achievable performance of a free convection cell if liquid water formation were prevented.

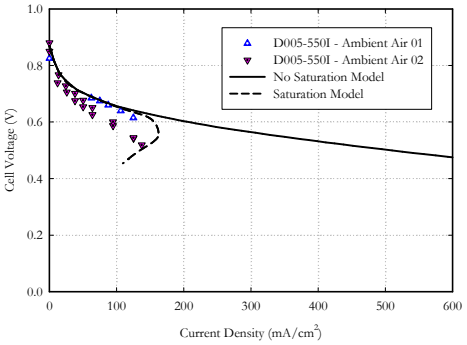

Figure 9: Comparison of Models and Experiment

V. FUTURE WORK

Next generation devices are currently being designed with feature geometry and wetting characteristics that will minimize mass transport resistances associated with product water blocking active sites. Future micromachined GDM structures will be tailored to (1) effectively separate reactant gas and liquid phase mass transport, (2) prevent flooding of the catalyst layer at low cell temperatures (<40°C), (3) minimize contact losses and (4) prevent membrane dryout.

VI. CONCLUSIONS

Component level design, fabrication, test and modeling studies have been carried out for micromachined GDM structures applicable for small, free-convection PEM fuel cells. The devices, though simple in design, have succeeded in replacing conventional carbon cloth or paper GDM's with micro-machined versions having slightly lower performance. Supplemental modeling has provided insight into the operability and theoretical maximum performance of the cell, suggesting dramatic improvements if liquid water formation were prevented.

V. ACKNOWLEDGMENTS

Special thanks to Akilesh Sridharan for his support in the fabrication effort and wafer fabrication database development. Discussions and contributions of Professor Scott Barton, Professor Alan West and Dr. Arthur Kaufman are greatly appreciated. The authors gratefully acknowledge the support of Columbia University's Mechanical Engineering Department.

REFERENCES

[1] Lee, S.J., Cha, S.C., Liu, Y. , O'Hayre, R., Prinz, F.B., "High Power-Density Polymer-Electrolyte Fuel Cells By Microfabrication." Proceedings Volume 2000-3, The Electrochemical Society Proceeding Series, Pennington, NJ,

[2] Meyers, J.P., Maynard, H.L. "Design Considerations for Miniaturized PEM Fuel Cells." Journal of Power Sources, Vol. 109, pp 76-88, 2002.

[3] Kelley, S.C., Deluga, G.A., Smyrl, W.H. "Miniature Fuel Cells Fabricated on Silicon Substrates." Materials, Interfaces, and Electrochemical Phenomena. Vol. 48, No. 5 pp 1071-1082, May 2002.

[4] Vielstich, W., Lamm, A., Gasteiger, H.A. (editors) "Handbook of Fuel Cells." John Wiley & Sons, 2003.